Power Control for Cell-Edge User in NOMA Ultra Dense Networks

Sinh Cong LAM [1], Nam Hoang NGUYEN [1], Trong Minh HOANG [2], Kumbesan SANDRASEGARAN [3]

[1] Faculty of Electronics and Telecommunication, VNU University of Engineering and Technology,Vietnam
[2] Telecommunication Faculty No. 1, Posts and Telecommunications Institute of Technology, Vietnam
[3] International School of Engineering, Faculty of Engineering, Chulalongkorn University, Thailand

hoangtrongminh@ptit.edu.vn

Submitted April 29, 2025 / Accepted July 13, 2025 / Online first August 4, 2025

Abstract. *Adjusting user transmission power is an effective approach to managing Inter-Cell Interference (ICI) in Ultra-Dense Networks (UDNs). Thus, users can proactively adjust their transmission power to minimize total power consumption while maintaining the required quality-of-service. Most recent research on power control mechanisms focuses on designing policies that increase the transmission power for all active users, including both near users with good received signal qualities and far users with poor ones. However, since near users–referred to as Cell-Center Users (CCUs)–can already achieve the desired service quality, this paper applies the power control mechanism to far users, known as Cell-Edge Users (CEUs). The uplink coverage probabilities of near and far users are derived under the stretched path loss model and Rayleigh fading for systems with and without the power-domain Non-Orthogonal Multiple Access (NOMA) technique. The analysis shows that the proposed mechanism can significantly reduce transmission power by up to 25% in conventional systems and up to 36.6% in NOMA systems. Moreover, the NOMA system model with the proposed power control mechanism can also improve the ergodic capacity by up to 72.48%.*

Keywords

Power control, 5G, B5G, ultra dense networks, coverage probability, non-orthogonal multiple access

1. Introduction

The evolution of fifth-generation (5G) and beyond-5G (B5G) cellular networks is driving significant advancements in wireless communication technologies. One of the primary objectives of these emerging networks is to provide ubiquitous high quality-of-service across the entire coverage area. To fully fill these ambitious performance expectations, the deployment of UDNs, characterized by an extremely high density of BSs, has been recognized as a promising cellular network topology. This topology enhances spatial reuse of spectrum, reduces access delays, and improves network capacity, thereby supporting a wide range of data-intensive and latency-sensitive applications [1]. To allocate the spectrum for a large number of BSs in a small area, mmWave bands are considered the ideal carrier for UDNs due to their wide bandwidth availability. However, deploying BSs at extremely high density introduces significant challenges. Notably, mmWave signals are highly susceptible to obstacles and easily absorbed, resulting in significant power loss during transmission. Therefore, the users are encouraged to transmit at high power levels to ensure that the received signal power at the BSs is sufficient for further signal processing.

Due to the high density of BS deployment and the requirement of high user transmission power, uplink ICI management in UDNs has become a more significant challenge than in previous network topologies. Various techniques have been studied in the literature to mitigate ICI [2–4], advanced resource allocation using machine learning [5], and BS/user transmission power control [6], [7]. While conventional ICIC schemes rely on predefined criteria to group potential users or BSs into clusters [2], recent advanced Intercell Interference Coordination (ICIC) techniques leverage machine learning to address the joint BS resource allocation problem and power optimization. However, these solutions have their own limitations. For example, user/BS grouping techniques face challenges when the number of users and BSs randomly vary. Machine learning-based ICIC and resource allocation techniques also remain challenging due to their high computational cost. In that context, the power control technique in which the user and BS can proactively adjust their transmission power to meet the requirement for signal strength is still a potential solution.

By using a power control mechanism, users dynamically adjust their transmission power based on wireless channel conditions. Traditionally, users increase their transmission power in inverse proportion to the estimated path loss to their serving BS, thereby securing sufficient signal strength at the BS. Power control mechanisms have been extensively studied in the literature as one of the main challenges in cellular

DOI: 10.13164/re.2025.0554

systems [6], [8]. In [8], [9], the power control mechanism was discussed for the regular path loss model, where user transmission power is proportional to the path loss between the user and its serving BS or dynamically by the Artificial Bee Colony Algorithm. Based on a stochastic geometry framework, the uplink coverage probability of a user was derived for the multi-slope path loss model, which is characterized by multiple path loss exponents across different distance regimes. In recent work, the stretched path loss model has been proposed for UDNs as a simplified alternative to the conventional multi-slope model, where the path loss is computed using a single equation with only two tunable parameters [10]. The combination of power control mechanism and the NOMA technique was studied in [6], where the stretched path loss model was adopted to determine the user transmission power and analyse user performance.

Recently, machine learning has started being used to dynamically allocate the transmission power for users [7,11,12]. In [11], a Deep Reinforcement Learning technique was employed for a Cognitive Radio network, where the secondary user is unable to observe the transmission power level of the primary user. Thus, the secondary user must learn to adjust its transmission power to meet the quality-of-service requirements of both itself and the primary user. Dynamic power management on the secure broadcast channel was studied in [12], where an autonomous agent determines the transmission power for two users to prevent eavesdropping. In a recent work [7], a graph neural network was proposed for cellular systems to optimize power consumption and enhance spectrum utilization.

Although the aforementioned works have provided advanced techniques to dynamically control the user transmission power, they contain some limitations that should be addressed: (i) the power control schemes in these studies are designed for all active users. In UDNs utilizing mmWave, the signal qualities often widely vary as users randomly move within the coverage area. Specifically, some users are near the serving BSs and receive strong desired signals, allowing them to maintain the required quality of service even with lower transmission power. In contrast, others are far from the serving BSs and require much higher transmission power to achieve acceptable signal quality; (ii) Utilization of complex control algorithms can enhance user performance, but they may face challenges such as compatibility with cellular devices that have low computational capability and higher delays compared to conventional approaches.

To overcome these limitations, this paper focuses on a regular control approach in which the user proactively estimates path loss and individually adjusts its transmission power. Specifically, the paper defines CCUs and CEUs, where CCUs are near the serving BSs and CEUs are near the cell edges. Thus, the power control mechanism applies only to CEUs. The initial concept of this approach was presented in our recent work [13], where CCUs and CEUs are distinguished by channel conditions, particularly Line-of-Sight (LoS) and Non-LoS (NLoS) links. Since practical users cannot always accurately determine LoS/NLoS conditions, this paper classifies CCUs and CEUs based on the distance between the users and the serving BSs, which can be approximately estimated using reference signals [14]. In addition, the paper adopts the stretched path loss model, which generalizes the LoS/NLoS model, to make the results more general and less complex.

NOMA, which allows multiple users to simultaneously transmit on the same frequency band, is one of the core techniques in 5G and B5G systems [1]. NOMA can be applied in both the power domain and the code domain, where users sharing the same frequency band are distinguished by their transmission power or assigned codes, respectively. Although code-domain NOMA can support a large number of users concurrently, it typically requires significantly higher computational resources compared to power-domain NOMA. In UDNs with a large available mmWave spectrum, it is uncommon for multiple users to be assigned the same frequency band. Therefore, power-domain NOMA is still considered more feasible than code-domain NOMA in such scenarios. Most of works on the power-domain NOMA technique focus on pairing two appropriate users to perform frequency band sharing. Conventionally, the BS usually pairs a good channel quality user, i.e. near user, with a bad channel condition, i.e. far user [15–17]. In a such manner, the far user is able to employ a higher transmission power than the near user. In [18], a novel user pairing scheme is proposed for an Integrated Sensing and Communication system with cooperative NOMA to maximize the achievable sum rate of users. Specifically, the channel orthogonality is used together with correlation among users to determine the pair of users. For cellular networks-assisted Unmanned Aerial Vehicle, the authors in [19] discussed a two-hop user grouping to maximize the system sum rate. Furthermore, the joint optimization between the user pairing and other problems such as beam forming, transmission power minimization [20], [21] and reflection coefficient of simultaneously transmitting and reflecting reconfigurable intelligent surface [22]. Through the discussed papers, it can be stated that research on power-domain NOMA, particularly in finding an appropriate pair of users, is still an open topic and requires further investigation.

Therefore, the paper combines the power control mechanism and power-NOMA technique in a simple manner. Specifically, a user that is farther than reference distance R is called CCU, and a user with larger distance is CEU. The highlighted contributions of the paper are as follows:

- Instead of applying a power control mechanism to all users, the paper proposes utilizing this mechanism for CEUs only. Under this policy, the transmission powers of the CCU and CEU are P_0 and $P_0 \exp\left(\epsilon \alpha r^{\beta}\right)$, respectively, where P_0 denotes the minimum user transmission power. This approach also incorporates the ICIC technique, which allows CEUs to transmit at a higher power level than CCUs.

- Based on the definition of CCU and CEU, the paper employs the power-domain NOMA technique so that this pair of CCU-CEU is able to simultaneously utilize the same frequency band. Specially, the CEU acts as the far user and control its transmission power by the power control mechanism.
- The coverage probabilities of the CCU (without power control) and the CEU (with power control) in the system with and without the power-domain NOMA technique are derived under a stretched path loss model and Rayleigh fading.
- The analytical results indicates that the proposed power control mechanism can significantly save the power consumption for both the system with and without power-domain NOMA technique.

In comparison with advanced approaches such as machine learning or Artificial Bee Colony algorithm, the proposed mechanism has higher feasibility. Specifically: (i) It is based on the distance between the user and its serving BS, which is determined by the network without advanced techniques; (ii) It requires neither data and hardware as in machine learning-based algorithms, nor a high computational load like the Artificial Bee Colony algorithm; (iii) It can operate in real-time.

2. System Model

This study investigates indoor cellular networks in which BSs and users are randomly positioned within the coverage area, following a Spatial Poisson Point Process (PPP). All BSs share the entire available bandwidth, i.e. full frequency reuse. Moreover, the user density is assumed to be sufficiently high such that every BS has at least two active users, as illustrated in Fig. 1.

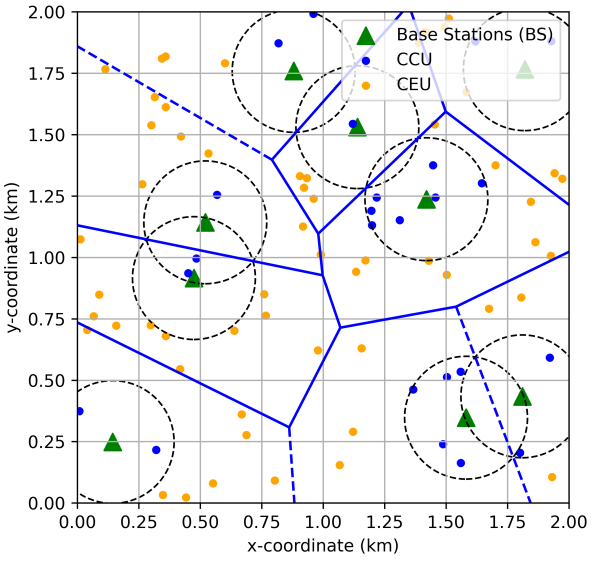

Fig. 1. System model.

The user utilizes the nearest-association strategy, where it identifies and sends a communication request to the closest active BS. Thus, the distance between the user and its serving BS has the following Probability Density Function (PDF):

$$f_R(r) = 2\pi\lambda r \exp(-\pi\lambda r^2) \tag{1}$$

where λ is the density of BSs.

In densely populated environments with a high concentration of obstacles such as humans, furniture, walls, and so on, the user-BS link is frequently blocked. Therefore, instantaneous channel gain can be modelled by Rayleigh random variable. As the result, the channel power gain has a unit exponential distribution. In addition, the signal also suffers path loss which can be captured through stretched path loss model. According these models, the path loss over a distance of r is

$$L(r) = \exp(-\alpha r^{\beta}) \tag{2}$$

where α and β are determined by the obstacle properties. Specifically, β depends the density of obstacles while α captures the radio attenuation characteristics of these obstacles.

2.1 Proposed Power Control Mechanism

The power control mechanism is designed to compensate path loss, ensuring that the signal strength remains within an acceptable range while also reducing ICI with other users. Conventionally, this mechanism increases the user transmission power by an amount proportional to the path loss. In dB, the transmission power of the user is

$$P_{\mathrm{u}}[\mathrm{dB}] = P_0[\mathrm{dB}] + \epsilon / L(r)[\mathrm{dB}] \tag{3}$$

where P_0 is the standard/minimum user transmission power; ϵ is the power control coefficient ($0 \leq \epsilon \leq 1$).

In the complex indoor transmission conditions with various obstacles, the received mmWave signal power significantly depends on the transmission distances and density of obstacles. Therefore, the path loss may dynamically vary with both time and distance. Meanwhile, the user's position only slightly changes during the transmission duration. Hence, this paper adopts the power control mechanism based on the distance between the user and its BS rather than on the path loss. The transmission power of the user is defined as

$$P_{\mathrm{u}} = P_0 L_{\epsilon}(r) = P_0 \exp\left(\alpha r^{\epsilon\beta}\right). \tag{4}$$

Due to variance of the received signal strength, some users with the low path loss can achieve the desired signal powers without any advanced techniques while others with serious path loss and require the power control mechanism to enhance the received signal strength. Thus, the paper proposes to employ the power control mechanism for the users with critical path loss only, i.e the user is farther than the reference distance of R or CEU. Meanwhile, the CCU utilizes the fixed power during its transmission.

The proposed power control mechanism can be applied in practical networks. Specifically, the classification of CCUs and CEUs is feasible since the BS can accurately estimate the positions of its associated users. Based on the analysis of various network conditions in Sec. 5, the BS can then select the most appropriate power control coefficient ϵ and assign it to the CEUs via signaling messages.

Mathematically, the user at distance r from its serving BS is called a near user or CCU if $r < R$. Since r is the distance from the user to its nearest BS, the PDF of r is $f_R(r) = 2\pi\lambda \exp(-\pi\lambda r^2)$. Let $\mathbf{1}(r < R)$ is the indicator function that takes a value of 1 if $r < R$ and 0 if $r \geq R$. Thus, the expectation of $\mathbf{1}(r < R)$ is

$$\begin{aligned}\mathbb{E}\left(\mathbf{1}(r < R)\right) &= \int_0^R 2\pi\lambda r \exp(-\pi\lambda r^2)\mathrm{d}r \\ &= 1 - \exp\left(-\pi\lambda R^2\right). \end{aligned} \tag{5}$$

Consequently, the transmission power of the user can be rewritten as follows:

$$P_{\mathrm{u}}(r) = \begin{cases} P_0 & \text{for CCU or } r < R \\ P_0 L_\epsilon(r) & \text{for CEU or } r > R \end{cases}. \tag{6}$$

The transmission power of the randomly distributed user at a distance of r from its serving BS is

$$P(r) = \mathbf{1}(r < R)P + \mathbf{1}(r > R)\exp\left(\alpha r^{\epsilon\beta}\right). \tag{7}$$

By taking the expectation with respects to r, the average transmission power of this user is

$$\begin{aligned} P(r) =& \mathbb{E}\left[\mathbf{1}(r < R)P_0 + \mathbf{1}(r > R)P_0 \exp\left(\alpha r^{\epsilon\beta}\right)\right] \\ =& \int_0^R 2\pi\lambda r P_0 \exp(-\pi\lambda r^2)\mathrm{d}r \\ &+ \int_R^\infty 2\pi\lambda r P_0 \exp\left(\alpha r^{\epsilon\beta}\right)\exp(-\pi\lambda r^2)\mathrm{d}r\mathrm{d}r \\ =& \left[1 - \exp\left(-\pi\lambda R^2\right)\right] P_0 \\ &+ \int_R^\infty 2\pi\lambda r P_0 \exp\left(\alpha r^{\epsilon\beta}\right)\exp(-\pi\lambda r^2)\mathrm{d}r. \end{aligned} \tag{8}$$

2.2 Uplink SINR without NOMA

With the transmission power as in (6), the desired signal power at the BS of the CCU and CEU are respectively

$$P_{\mathrm{u}}(r) = \begin{cases} P_0 g L(r) & \text{for CCU or } r < R \\ P_0 g L(r) L_\epsilon(r) & \text{for CEU or } r > R \end{cases} \tag{9}$$

where g is the instantaneous channel power gain.

In the UDNs with very high density of BSs, the BSs independently perform resource allocation mechanism for all their active users. When the number of users is large enough, it is highly possible that a given frequency band can be simultaneously occupied by all BSs. Thus, the typical user suffers ICI from all adjacent BSs. In every BS of the system without NOMA technique, a given frequency band is only used by one user. Consequently, the number of interfering sources of the typical user is exactly the number of BSs whose density is λ.

Let d_j and r_j are distance from the interfering user j to its serving BS and serving BS of the user, respectively. The transmission power of user j is determined by the power control mechanism in (6). Particularly,

$$P_{\mathrm{u}}(d_j) = \begin{cases} P_0 & \text{if } d_j < R \\ P_0 L_\epsilon(d_j) & \text{if } d_j > R \end{cases} \tag{10}$$

and the interfering power at the serving BS of the typical user is

$$I_j(r_j) = \begin{cases} P_0 L(r_j) & \text{if } d_j < R \\ P_0 \frac{L(r_j)}{L^\epsilon(d_j)} & \text{if } d_j > R \end{cases}. \tag{11}$$

The total uplink ICI of the typical user is

$$I = P_0 \sum_{j\in\theta} g_j L(r_j)\left[\mathbf{1}(d_j < R) + L_\epsilon(d_j)\mathbf{1}(d_j > R)\right] \tag{12}$$

where g_j is the instantaneous channel power gain from interfering user j to the serving BS of the typical user. Consequently, the uplink SINR of the typical user is:

$$SINR = \begin{cases} \dfrac{P_0 g L(r)}{I + \sigma^2} & \text{for CCU or } r < R \\ \dfrac{P_0 g L(r) L_\epsilon(r)}{I + \sigma^2} & \text{for CEU or } r > R \end{cases} \tag{13}$$

where σ^2 is the power of Gaussian noise.

2.3 Non-Othorgonal Multiple Access

When the power-domain NOMA technique is employed, each BS looks for a pair of users to assign the same frequency band. Therefore, the BS distinguishes the transmitted signals of these users by analysing their signal powers. The paper assumes that each user group comprises a CCU and a CEU. In comparison with system without NOMA where the frequency band is occupied either CCU or CEU, the CCU signal at the BS in the NOMA system is affected by ICI from CEU and vice versa due to share of frequency band. However, this ICI can be removed by Successive Interference Cancellation (SIC) technique. Thus, this paper only studies the ICI. Since the frequency band is simultaneously utilized a pair of CCU-CEU, the total ICI on a given frequency band is

$$I_{\mathrm{NOMA}} = P_0 \sum_{j\in\theta} g_j L(r_j) + P_0 \sum_{j\in\theta} g_j L(r_j) L_\epsilon(d_j) \tag{14}$$

where $P_0 \sum_{j\in\theta} g_j L(r_j)$ is the total ICI from the interfering CCUs whose transmissions are P_0; $P_0 \sum_{j\in\theta} g_j L(r_j) L_\epsilon(d_j)$ is the ICI that is originated from CEUs with transmission powers of $P_0 L_\epsilon(d_j)$.

Since the utilization of NOMA technique only causes the change in ICI, the desired signal of CCU and CEU are still obtained from (9). Therefore, the uplink SINR in the NOMA system is

$$SINR_{\text{NOMA}} = \begin{cases} \dfrac{P_0 g L(r)}{I_{\text{NOMA}} + \sigma^2} & \text{for CCU} \\ \dfrac{P_0 g L(r) L_\epsilon(r)}{I_{\text{NOMA}} + \sigma^2} & \text{for CEU} \end{cases}. \quad (15)$$

3. Performance Analysis

3.1 Laplace Transform of ICI

The Laplace transform of ICI is defined as

$$\mathcal{L}(s) = \mathbb{E}\left[\exp(-sI)\right] \quad (16)$$

Theorem 3.1 The Laplace transform of ICI in the system without NOMA is $\mathcal{L}(s) =$

$$\exp\left(-2\pi\lambda \int_0^R \int_{d_j}^\infty \frac{sP_0 L(r_j)}{1+L(r_j)} r_j \mathrm{d}r_j f_R(d_j)\mathrm{d}d_j\right) \times \exp\left(-2\pi\lambda \int_R^\infty \int_{d_j}^\infty \frac{sP_0 \frac{L(r_j)}{L^\epsilon(d_j)} r_j}{1+sP_0\frac{L(r_j)}{L^\epsilon(d_j)}} \mathrm{d}r_j f_R(d_j)\mathrm{d}d_j\right). \quad (17)$$

Proof 3.2 Since I is a function of random variables such as the distance between user and BSs, channel power gains, number of BSs, its Laplace transform is evaluated by the following steps. Substituting the definition of ICI in (12), we obtains $\mathcal{L}(s)$

$$= \mathbb{E}\left[\exp\left[-s\left(P_0 \sum_{j\in\theta} g_j L(r_j) \begin{bmatrix} \mathbf{1}(d_j < R) + \\ L_\epsilon(d_j)\mathbf{1}(d_j > R) \end{bmatrix}\right]\right]\right]$$

$$= \mathbb{E}\begin{bmatrix} \exp\left[-s\left(P_0 \sum_{j\in\theta} g_j L(r_j)\mathbf{1}(d_j < R)\right)\right] \\ \exp\left[-s\left(P_0 \sum_{j\in\theta} g_j L(r_j) L_\epsilon(d_j)\mathbf{1}(d_j > R)\right)\right] \end{bmatrix}.$$

Since all instantaneous channel power gains are independent random variables, and $\mathbf{1}(d_j < R)$ and $\mathbf{1}(d_j > R)$ are two exclusive events, the Laplace transform can be simplified as

$$\mathcal{L}(s) = \mathbb{E}\begin{bmatrix} \prod_{j\in\theta} \exp\left(-sP_0 g_j L(r_j)\mathbf{1}(d_j < R)\right) \\ \prod_{j\in\theta} \exp\left[-sP_0 g_j L(r_j) L_\epsilon(d_j)\mathbf{1}(d_j > R)\right] \end{bmatrix}$$

$$= \mathbb{E}\begin{bmatrix} \prod_{j\in\theta} \mathbb{E}\left[\exp\left(-sP_0 g_j L(r_j)\mathbf{1}(d_j < R)\right)\right] \\ \prod_{j\in\theta} \mathbb{E}\left[\exp\left[-sP_0 g_j L(r_j) L_\epsilon(d_j)\mathbf{1}(d_j > R)\right]\right] \end{bmatrix}.$$

Since $\mathbf{1}(d_j < R)$ and $\mathbf{1}(d_j > R)$ are indicator functions whose the expectation of Laplace transform $E[-a\mathbf{1}(x)] = 1 - \mathbb{E}(x)(1-a)$, $\mathcal{L}(s)$ is equal to

$$\mathcal{L}(s) = \mathbb{E}\begin{bmatrix} \prod_{j\in\theta} \left(1 - \left(1 - \exp\left(-sP_0 g_j L(r_j)\right)\right) \middle| d_j < R\right) \\ \prod_{j\in\theta} \left(1 - \left(1 - \exp\left(-sP_0 g_j \frac{L(r_j)}{L^\epsilon(d_j)}\right)\right) \middle| d_j > R\right) \end{bmatrix}.$$

Due to the independence of instantaneous channel power gains whose expectation of Laplace transform is $\mathrm{E}[\mathrm{e}^{-gs}] = \frac{1}{1+s}$, the Laplace transform of ICI is obtained by

$$\mathcal{L}(s) = \mathbb{E}\begin{bmatrix} \prod_{j\in\theta} \left[1 - \frac{sP_0 L(r_j)}{1+sP_0 L(r_j)} \middle| d_j < R\right] \\ \prod_{j\in\theta} \left[1 - \frac{sP_0 \frac{L(r_j)}{L^\epsilon(d_j)}}{1+sP_0 \frac{L(r_j)}{L^\epsilon(d_j)}} \middle| d_j > R\right] \end{bmatrix}. \quad (18)$$

It is recalled that the distance from the interfering user to the victim BS is greater than that to its serving BS, $r_j > d_j$ whose PDF $f(d_j) = 2\pi\lambda \exp\left(-\pi\lambda d_j^2\right)$. Therefore, the above expectation with respect to d_j is evaluated as:

$$\mathcal{L}(s) = \mathbb{E}\begin{bmatrix} \prod_{j\in\theta} \left[1 - \int_0^\infty \frac{sP_0 L(r_j)}{1+sP_0 L(r_j)} f_R(d_j)\mathrm{d}d_j\right] \\ \prod_{j\in\theta} \left[1 - \int_R^\infty \frac{sP_0 \frac{L(r_j)}{L^\epsilon(d_j)}}{1+sP_0 \frac{L(r_j)}{L^\epsilon(d_j)}} f_R(d_j)\mathrm{d}d_j\right] \end{bmatrix}. \quad (19)$$

The above expectation can be obtained by using the Properties of Generating Function which states that $\mathbb{E}\left[\prod_{j\in\theta} f(x)\right] = \exp\left(-2\pi\lambda \int_x (1-f(x))x\mathrm{d}x\right)$. Thus, the Laplace transform is obtained as in (17).

Theorem 3.3 The Laplace transform of ICI in the system without NOMA is $\mathcal{L}_{\text{NOMA}}(s) =$

$$\exp\left(-4\pi\lambda \int_0^R \int_{d_j}^\infty \frac{sP_0 L(r_j) r_j}{1+sP_0 L(r_j)} \mathrm{d}r_j f_R(d_j)\mathrm{d}d_j\right) \times \exp\left(-4\pi\lambda \int_R^\infty \int_{d_j}^\infty \frac{sP_0 \frac{L(r_j)}{L^\epsilon(d_j)} r_j}{1+\frac{L(r_j)}{sP_0 L^\epsilon(d_j)}} \mathrm{d}r_j f_R(d_j)\mathrm{d}d_j\right). \quad (20)$$

Proof 3.4 The main difference between the system with and without NOMA refers to the re-use of frequency band within a cell. In the system without NOMA, each frequency band is only used one user while the NOMA system allows a pair of users simultaneously transmit on the same frequency band. Thus, the density of interfering users in the system without NOMA is λ while that in the system with NOMA is 2λ. Therefore, the Laplace transform of the ICI power in the NOMA system is obtained from (20).

3.2 Coverage Probability

To examine the performance of the proposed power control mechanism, the probability that the user is under the coverage of its nearest BS, i.e. coverage probability, is studied. For both the system with and without NOMA, the

coverage probability of the user with the coverage threshold of T is defined as the conditional probability

$$\mathcal{P}(T) = \mathbb{P}\left(SINR > T\right) \tag{21}$$

where $SINR$ is defined in (13) and (15) for the system without and with NOMA technique, respectively.

For CCU The coverage probability of the CCU in the system without NOMA technique is given by

$$\begin{aligned}\mathcal{P}_{\mathrm{c}}(T) &= \mathbb{P}\left(\frac{P_0 g L(r)}{I+\sigma^2} > T\right) \\ &= \mathbb{P}\left(g > T\frac{I}{P_0 L(r)} + T\frac{1}{\gamma L(r)}\right)\end{aligned} \tag{22}$$

where $\gamma = \frac{P_0}{\sigma^2}$. Under multipath condition as Rayleigh random variable, the channel power gain is an exponential random variable with CDF distribution $F(g) = \exp(-g)$, the CCU coverage probability is

$$\mathcal{P}_{\mathrm{c}}(T) = \mathbb{E}\left[\exp\left(-T\frac{1}{\gamma L(r)}\right)\mathcal{L}\left(\frac{T}{P_0 L(r)}\right)\right]. \tag{23}$$

Since the distance of the CCU is a random variable which varies from $(0; R)$ and its PDF is given by (1), the coverage probability is finally obtained by

$$\mathcal{P}_{\mathrm{c}}(T) = \int_0^R \exp\left(-T\frac{1}{\gamma L(r)}\right)\mathcal{L}\left(\frac{T}{P_0 L(r)}\right) f_R(r)\mathrm{d}r. \tag{24}$$

For CEU Similarity, the coverage probability of CEU in the system without NOMA technique is obtained by $\mathcal{P}_{\mathrm{e}}(T)$

$$\begin{aligned}&= \mathbb{P}\left(\frac{P_0 g L(r) L_\epsilon(r)}{I+\sigma^2} > T\right) \\ &= \int_R^\infty \exp\left(-\frac{T L_\epsilon^{-1}(r)}{\gamma L(r)}\right)\mathcal{L}\left(\frac{T L_\epsilon^{-1}(r)}{P_0 L(r)}\right) f_R(r)\mathrm{d}r.\end{aligned} \tag{25}$$

Random user When the user is randomly located in the network area and has a distance of r to its serving BS, it can be CCU if $r < R$ and CEU if $r > R$. Thus, the coverage probability of the random user is

$$\mathcal{P}(T) = \mathcal{P}_{\mathrm{c}}(T) + \mathcal{P}_{\mathrm{e}}(T). \tag{26}$$

For the NOMA system, the coverage probabilities of the CCU, CEU and random user are obtained from (24), (25) and (26) by substituting $\mathcal{L}(s)$ with $\mathcal{L}_{\mathrm{NOMA}}(s)$.

[1]https://github.com/congls/radioEng.git

4. Ergodic Capacity

The uplink ergodic capacity of the user in the cellular network with unit bandwidth is defined by the Shannon theorem which states that

$$C = \log_2(1 + SINR) \tag{27}$$

where $SINR$ is the uplink SINR of the user. Since $SINR$ is a random variable, the ergodic capacity in the system without NOMA can re-written in the following form

$$C = \mathbb{E}\left[\log_2(1+SINR)\right] = \int_0^\infty \mathbb{E}\left[SINR > \mathrm{e}^t - 1\right]\mathrm{d}t.$$

Since the frequency band in the NOMA system is occupied by a pair of CCU-CEU, the ergodic capacity in the NOMA system is the sum of the CCU capacity C_{CCU} and CEU capacity C_{CEU}. Therefore,

$$C_{\mathrm{NOMA}} = C_{\mathrm{CCU}} + C_{\mathrm{CEU}}. \tag{28}$$

5. Simulation and Analysis

In this section, the simulation results are derived to provide a clearly examination of the proposed system model.

5.1 Theoretical Validation

To validate the analytical results in (26), the following indoor network scenario is adopted:

- In the indoor environment with high density of walls, the BS can cover one or two rooms which corresponds to the coverage area of about $10\,\mathrm{m}^2$. Thus, the simulation assumes that the density of BSs $\lambda = 0.1 \cdot 10^6$ BS/m^2 [1].
- The transmission conditions is characterized by the density of obstacles $\beta = 1$ and their radio attenuation coefficient $\alpha = 0.5$. In that scenario, the density of obstacles on each link are proportional to the length of that link. This assumption is suitable for office corridors with small rooms facing each other.
- The power control coefficient is set to $\epsilon = 0.1$, and the SNR is varied as $\gamma = -20, -10, 10, 20$ dB. These values are used to evaluate the performance of the proposed system under different signal conditions, ranging from very poor to good.

In addition, the network area and Monte Carlo iteration are chosen to be as large as possible. Larger value of these parameters give the higher accurate and stable results. Specifically, the network area is covered by a circular with the radius of 2000 m; the number of Monte Carlo iteration is 10^5. All theoretical and simulation results are derived using computer programs written in Python [1].

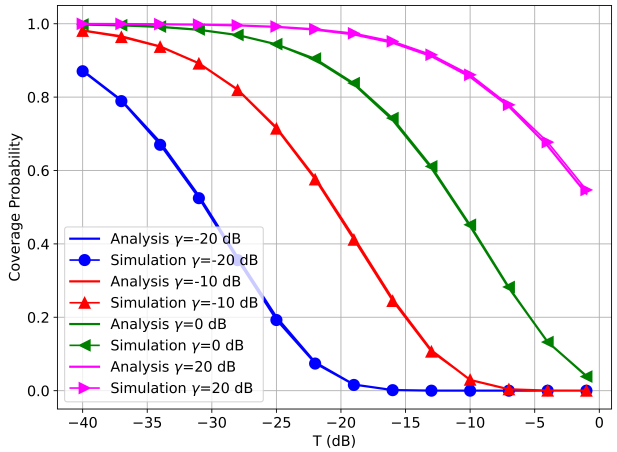

Fig. 2. Coverage probability vs coverage threshold.

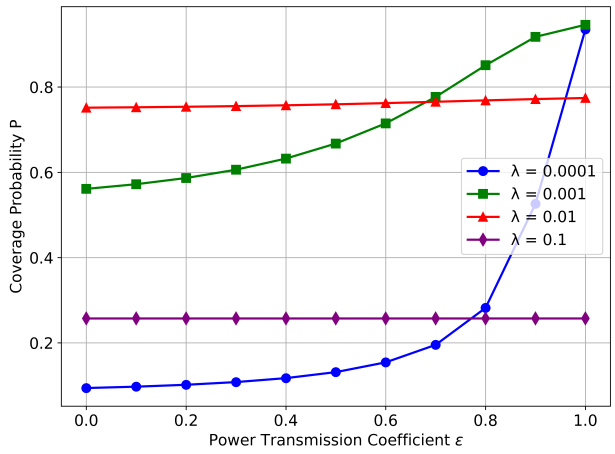

Fig. 3. Coverage probability vs power control exponent.

Figure 2 illustrates that Monte Carlo simulation results closely match the corresponding analytical results from (26). Thus, the derived theoretical analysis can be verified in terms of accuracy. The figure shows that at small values of SNR such as $SNR = -20\,\text{dB}$, an increase in SNR has a critical benefit to the user coverage probability. Meanwhile at high values of SNR, the changes of this parameter only reflects a small variance of user coverage probability. Take the 10 dB increase in SNR and coverage threshold $T = -25\,\text{dB}$ as an example, when SNR rises from –20 dB to –10 dB, the coverage probability increases by 250% from 0.2 to 0.7 while this performance metric only has a slight improvement of 36% from 0.7 to 0.95 as SNR increase from –10 dB to 0 dB.

5.2 Coverage Probability vs Power Control Coefficient

Figure 3 depicts the impact of the power control coefficient ϵ on the user coverage probability, under the assumption of $SNR = 10\,\text{dB}$, a target SINR threshold $T = -10\,\text{dB}$, and BS densities of $\lambda = 0.0001, 0.001, 0.01$ and $0.1\,\text{BS/m}^2$. Meanwhile $\lambda = 0.01$ and $\lambda = 0.1$ are considered the high values, two others are called the low ones. The analytical results are presented for the reference distance of $R = 10\,\text{m}$. Since an increase in ϵ directly translates to an escalation in the user transmission power, both the desired and ICI powers increase with ϵ. However, the effect of increasing ϵ on user performance exhibits contrasting behaviours depending on the level of network densification, i.e. the value of λ.

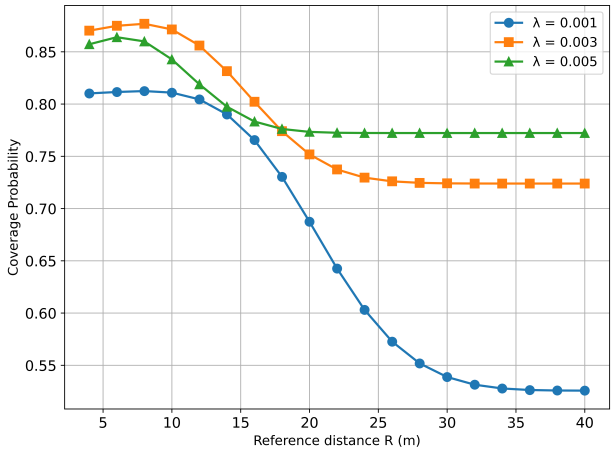

Fig. 4. Coverage probability vs reference distance R.

For a cellular network with a high density of BSs ($\lambda = 0.1; 0.01\,\text{BS/m}^2$), the network can be in a balanced state where the uplink SINR remains unchanged despite variations in user transmission power. As a result, the user coverage probability becomes independent of the power control coefficient. Specifically, Figure 3 shows that increasing the transmission power coefficient leads to only an infinitesimal change in the user coverage probability.

For a cellular network with a high density of BSs ($\lambda = 0.0001; 0.001\,\text{BS/m}^2$), most interfering signals travel long distances before colliding with the desired signal at the victim BS. As a result, these signals suffer significant path loss, and the interfering power is relatively small. Meanwhile, the desired signal only needs to travel a significantly shorter distance and therefore experiences lower path loss. As a result, increasing the power control coefficient and consequently the transmission power has a limited impact on interfering power but can significantly enhance the strength of the desired signal. Consequently, the SINR and user coverage probability increase.

5.3 Coverage Probability vs Reference Distance R

Figure 4 analyses the effects of reference distance R on the coverage probability in there network scenarios with $\lambda = 0.001; 0.03; 0.005\,(\text{BS/m}^2)$. Since the user that is farther than reference distance R utilizes the power control mechanism, the probability that the random distributed user utilizes the power control mechanism increases with R. Interestingly, for different network scenarios, the figure shows similar trends on the coverage probability.

It is recalled that the CEU classification probability is given by $\exp(-\pi\lambda R^2)$, which decreases exponentially as R increases. For small values of R, most users are classified as CEUs and utilize the power control mechanism to adjust their transmission powers. When R increases from 5 m to 10 m in a network with a density of $\lambda = 0.001$ BS/m^2, the CEU probability decreases from approximately 0.92 to 0.73 (a 26% reduction). This decline implies that fewer users are CEUs, resulting in a lower number of high-power interferers and, consequently, reductions in both the desired signal power and the ICI power. However, due to the balance between these signal powers, the coverage probability shows only slight variation for all values of λ as the reference distance increases from 4 m to 10 m. Notably, the user coverage probability in the network with $\lambda = 0.003$ remains around 0.87, despite a 26% reduction in CEU classification. Furthermore, it is observed that at $R = 4$ m and $R = 10$ m, the average transmission power of the user (obtained from (8)) is $2.0P_0$ and $1.6P_0$, respectively. Thus, it can be stated that the proposed model can save approximately 25% in power consumption while maintaining user coverage probability.

However, when the reference distance R exceeds 10 m, the CEU probability decreases more rapidly compared to smaller values of R. At this point, nearly all users become CCUs and transmit at the low power level. Therefore, further increases in R no longer significantly reduce ICI but instead substantially degrade the desired signal. As a result, the coverage probability begins to decline at large values of R. For instance, when the reference distance increases from 15 m to 20 m, the user coverage probability in the case of $\lambda = 0.003$ BS/m^2 drops by 9.3%, from 0.82 to 0.75, and by 13%, from 0.78 to 0.39, in the case of $\lambda = 0.001$ BS/m^2. This sharp decline at lower BS densities (e.g., $\lambda = 0.001$) indicates that the power control mechanism is more beneficial in low-density networks compared to those with higher densification.

At very large values of reference distance R such as $R > 25$ m in the cases of $\lambda = 0.002, 0.003$, and 0.005 BS/m^2, and 40 m in the case of $\lambda = 0.001$ BS/m^2 the CEU classification probability reaches its maximum value of 1, meaning that all users employ the power control mechanism. Therefore, as R continues to increase beyond these thresholds, the number of CEUs remains constant, and no further changes are observed in coverage probability behavior.

5.4 Ergodic Capacity vs Reference Distance R in NOMA System

Figure 5 illustrates the ergodic capacity in the proposed NOMA system as a function of the reference distance R, under two different channel conditions and two access schemes, with a fixed base station density $\lambda = 0.001$ BS/km^2. Two channel environments are considered: an acceptable one with $(\alpha = 0.125, \beta = 1)$ and a harsher one with $(\alpha = 0.25, \beta = 1.25)$. It can be seen that the utilization of the power-domain NOMA technique can significantly improve the data rate.

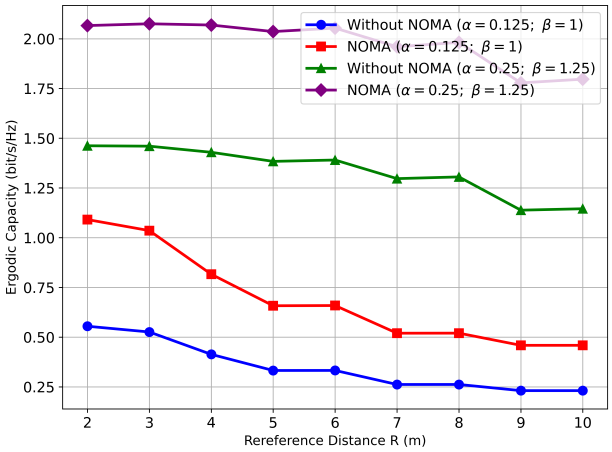

Fig. 5. Ergodic capacity vs reference distance R.

For $(\alpha = 0.125, \beta = 1)$, the ergodic capacity in the system without NOMA technique experiences a decline of about 60% from approximately 0.55 bit/s/Hz at $R = 2$ m to 0.22 bit/s/Hz at $R = 10$ m. In the system with the NOMA technique, the capacity drops about a similar percentage from 1.10 bit/s/Hz to 0.45 bit/s/Hz as the reference distance R decreases within the same range. It is valuable to note that for all values of R, the data rate in the proposed system maintains a twofold improvement over the regular system without NOMA technique.

In the harsher environment $(\alpha = 0.25, \beta = 1.25)$, the impact of NOMA deployment remains significant. At $R = 2$ m, the capacity without NOMA is 1.46 bit/s/Hz, while the system with NOMA achieves 2.05 bit/s/Hz, representing a 40% increase. At $R = 10$ m, the improvement widens to approximately 56.5%.

To examine more clearly the benefits of the proposed MONA system model on the user performance, Figure 6 plots the ergodic capacity with different values of ϵ and R in the network with the density of BSs $\lambda = 0.003$ BS/km^2. For small values of the reference distance R, nearly all users are classified as CEUs and operate under the power control mechanism. Specifically, at $R = 2$ m, the CEU classification probability is approximately 98.1%. Since the transmission power of all users increases with the power control coefficient, the user in the system with $\epsilon = 1$ experiences the highest level of ICI. Consequently, the ergodic capacity achieved for $\epsilon = 1$ is the lowest compared to the cases with $\epsilon = 0.4, 0.6$, and 0.8.

As the reference distance R increases, the probability that a user is classified as a CEU and thus activates the power control mechanism declines rapidly. For instance, at $R = 10$ m and $\epsilon = 1$, the CEU classification probability drops by about 37%, to approximately 61.5%, from its initial value at $R = 2$ m. This decline leads to a substantial reduction in overall ICI power, while the average desired signal power of both CCUs and CEUs experiences only a slight decrease. As a result, the ergodic capacity improves rapidly and reaches its peak. For example, in the case of $\epsilon = 1$, when $R = 12$ m

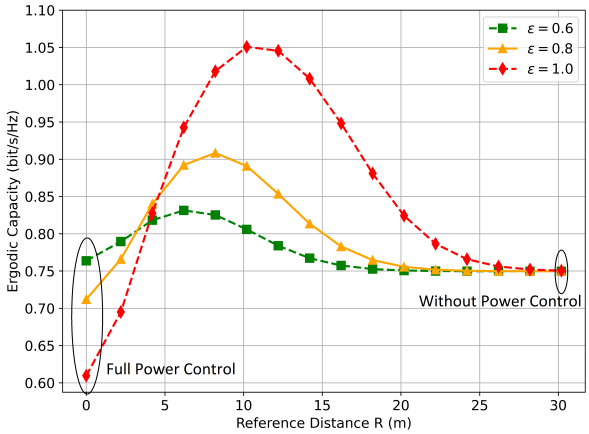

Fig. 6. Ergodic capacity vs reference distance R.

ϵ	Proposed model	Full power control		Without power control	
		Value	%	Value	%
0.6	0.8313	0.7637	8.85%	0.7496	10.91%
0.8	0.9083	0.7119	27.57%	0.7496	21.13%
1.0	1.0508	0.6094	72.48%	0.7504	40.03%

Tab. 1. Comparison of ergodic capacity of three NOMA systems.

(corresponding to a CEU probability of 22.93%), the ergodic capacity peaks at 1.05 bit/s/Hz representing a 72.48% increase compared to its value at $R = 0$ m. Furthermore, the average transmission power at $R = 0$ m and $R = 12$ m is $4.1P_0$ and $2.6P_0$, respectively. Hence, the proposed model can increase the ergodic capacity by up to 72.48% while reducing the average transmission power by 36.6%.

However, as the reference distance R continues to increase beyond 10 m in the case of $\epsilon = 1$, a different trend in ergodic capacity emerges. The CEU classification probability continues to decline, leading to a further decrease in the transmission power of interfering users and, consequently, in the total ICI power. However, in this range, the degradation of the desired signal becomes dominant. As a result, the ergodic capacity moderately decreases for all values of ϵ: when $R > 10$ m for $\epsilon = 1$, $R > 8$ m for $\epsilon = 0.8$, and $R > 6$ m for $\epsilon = 0.6$. For instance, when R increases from 12 m to 20 m, the ergodic capacity for $\epsilon = 1$ decreases from around 1.04 bit/s/Hz to approximately 0.83 bit/s/Hz, indicating a capacity loss of about 20%.

Table 1 compares the performance of the proposed system model with the full power control ($R = 0$) and without power control ($R = 30$) NOMA systems.

6. Conclusion

In this paper, a power control mechanism is proposed specifically for CEUs located beyond a reference distance of R from their serving BS. In this approach, CCUs use a fixed transmission power, while the transmission power of CEUs depends on the channel condition and the distance to their serving BS. The coverage probability of a randomly located user, either a CCU or a CEU, is derived under the stretched path loss model and Rayleigh fading. The analysis, conducted under varying network densities and power control coefficients, reveals several key findings. First, the utilization of the power control mechanism can significantly improve user performance under favorable channel conditions or in networks with small value of density of BSs λ. Second, in systems without NOMA technique, the proposed power control scheme can reduce power consumption by approximately 25% while maintaining acceptable user performance. Finally, in systems with the power-domain NOMA technique, the proposed model can enhance the ergodic capacity by up to 72.48% and simultaneously save up to 36.6% of transmission power. Although the proposed algorithm is simple and has a low computational load, it requires knowledge of the user's position to function accurately in real-time scenarios.

References

[1] JIANG, W., HAN, B., HABIBI, M. A., et al. The road towards 6G: A comprehensive survey. *IEEE Open Journal of the Communications Society*, 2021, vol. 2, p. 334–366. DOI: 10.1109/OJCOMS.2021.3057679

[2] SONG, M., SHAN, H., YANG, H. H., et al. Joint optimization of fractional frequency reuse and cell clustering for dynamic TDD small cell networks. *IEEE Transactions on Wireless Communications*, 2022, vol. 21, no. 1, p. 398–412. DOI: 10.1109/TWC.2021.3096383

[3] VAEZI, M., LIN, X., ZHANG, H., et al. Deep reinforcement learning for interference management in UAV-based 3D networks: Potentials and challenges. *IEEE Communications Magazine*, 2024, vol. 62, no. 2, p. 134–140. DOI: 10.1109/MCOM.001.2200973

[4] ONAY, M. Y. Dynamic time allocation based physical layer security for jammer-aided symbiotic radio networks. *Radioengineering*, 2024, vol. 33, no. 3, p. 442–451. DOI: 10.13164/re.2024.0442

[5] LIU, Y., ZENG, Z., TANG, W., et al. Data-importance aware radio resource allocation: Wireless communication helps machine learning. *IEEE Communications Letters*, 2020, vol. 24, p. 1392–1396. DOI: 10.1109/LCOMM.2020.2996605

[6] LAM, S. C., PHAM, T. H., TRAN, X. N. Uplink performance of nonorthogonal multiple access ultradense networks with power control. *International Journal of Communication Systems*, 2022, vol. 35, no. 6, p. 1–18. DOI: 10.1002/dac.5069

[7] MARWANI, M., KADDOUM, G. Graph neural networks approach for joint wireless power control and spectrum allocation. *IEEE Transactions on Machine Learning in Communications and Networking*, 2024, vol. 2, p. 717–732. DOI: 10.1109/TMLCN.2024.3408723

[8] DING, T., DING, M., MAO, G., et al. Uplink performance analysis of dense cellular networks with LoS and NLoS transmissions. *IEEE Transactions on Wireless Communications*, 2017, vol. 16, no. 4, p. 2601–2613. DOI: 10.1109/TWC.2017.2669023

[9] SREENU, S., KALPANA, N. Innovative power allocation strategy for NOMA systems by employing the modified ABC algorithm. *Radioengineering*, 2022, vol. 31, no. 3, p. 312–322. DOI: 10.13164/re.2022.0312

[10] ALAMMOURI, A., ANDREWS, J. G., BACCELLI, F. SINR and throughput of dense cellular networks with stretched exponential path loss. *IEEE Transactions on Wireless Communications*, 2018, vol. 17, no. 2, p. 1147–1160. DOI: 10.1109/TWC.2017.2776905

[11] ZHANG, H., YANG, N., HUANGFU, W., et al. Power control based on deep reinforcement learning for spectrum sharing. *IEEE Transactions on Wireless Communications*, 2020, vol. 19, no. 6, p. 4209–4219. DOI: 10.1109/TWC.2020.2981320

[12] ARVANITAKI, A., STAMATAKIS, G., CARLSSON, N., et al. Deep reinforcement learning for power control in secure broadcast channels. In *Proceedings of the 21st International Symposium on Modeling and Optimization in Mobile, Ad Hoc, and Wireless Networks (WiOpt)*. Singapore, 2023, p. 578–583. DOI: 10.23919/WiOpt58741.2023.10349852

[13] LAM, S. C., TRAN, D.-T., SANDRASEGARAN, K. Power control in uplink indoor ultra dense networks. In *Proceedings of the 22nd International Conference on Electrical Engineering/Electronics, Computer, Telecommunications and Information Technology (ECTI-CON)*. Bangkok (Thailand). 2025.

[14] ONAY, M. Y. Secrecy rate performance analysis of jammer-aided symbiotic radio with sensing errors for fifth generation wireless networks. *Applied Sciences*, 2025, vol. 15, no. 1, p. 1–22. DOI: 10.3390/app15010289

[15] ARSHAD, R., BAIG, S., ASLAM, S. User clustering in cell-free massive MIMO NOMA system: A learning based and user centric approach. *Alexandria Engineering Journal*, 2024, vol. 90, p. 183–196. DOI: 10.1016/j.aej.2024.01.064

[16] NASSER, A., CELIK, A., ELTAWIL, A. M. Joint user-target pairing, power control, and beamforming for NOMA-aided ISAC networks. *IEEE Transactions on Cognitive Communications and Networking*, 2025, vol. 11, no. 1, p. 316–332. DOI: 10.1109/TCCN.2024.3427781

[17] ZHAO, D., HU, L., XIONG, W., et al. On optimization of RIS-assisted secure UAV-NOMA communications with finite block-length. *Radioengineering*, 2024, vol. 33, no. 4, p. 526–536. DOI: 10.13164/re.2024.0526

[18] AMHAZ, A., ELHATTAB, M., ASSI, C., et al. Cooperative NOMA empowered integrated sensing and communication: Joint beamforming and user pairing. *IEEE Transactions on Cognitive Communications and Networking*, 2024, vol. 10, no. 6, p. 2164–2176. DOI: 10.1109/TCCN.2024.3414394

[19] GUO, X., LI, B., WU, J., et al. Joint uplink and downlink NOMA for UAV relaying network with multi-pair users. *IEEE Transactions on Wireless Communications*, 2024, vol. 23, no. 12, p. 18549–18562. DOI: 10.1109/TWC.2024.3470119

[20] DONG, Y., YANG, Z., WANG, H., et al. Joint user pairing and beamforming design for NOMA-aided CFMM-ISAC systems. *IEEE Internet of Things Journal*, 2025, vol. 12, no. 6, p. 6749–6763. DOI: 10.1109/JIOT.2024.3491137

[21] DUAN, S., LI, S., WEI, M., et al. Transmit power minimization for IRS-assisted full-duplex cooperative NOMA networks. In *Proceedings of the 24th International Conference on Communication Technology (ICCT)*. Chengdu (China), 2024, p. 468–473. DOI: 10.1109/ICCT62411.2024.10946572

[22] WU, Y., ZHANG, C., HAI, H., et al. Average sum-rate maximization of coupled phase-shift STAR-RIS-assisted SWIPT-NOMA system. *IEEE Communications Letters*, 2024, vol. 28, no. 12, p. 2889–2893. DOI: 10.1109/LCOMM.2024.3487981

About the Authors . . .

Sinh Cong LAM received the Ph.D. degree in Engineering from University of Technology, Sydney, Australia, in 2018. He has been working with the University of Engineering and Technology, Vietnam National University, Hanoi since 2010 where he was promoted to an Associate Professor in 2024. His research interests focus on modeling, performance analysis and optimization for 5G and B5G, stochastic geometry model for wireless communications

Nam Hoang NGUYEN received the Ph.D. degree from the Vienna University of Technology, Austria, in 2002. He has been working with the University of Engineering and Technology, Vietnam National University, Hanoi, since 2011, where he was promoted to an Associate Professor in 2018. His research interests include resource management for mobile communications networks and future visible light communications.

Trong Minh HOANG (corresponding author) earned bachelor's degrees in Physics Engineering (1994) and Electronic and Communications Engineering (1999) from Hanoi University of Science and Technology. His master's degree (2003) and Ph.D. degree (2014) in Electronic and Telecommunication Engineering from the Posts and Telecommunications Institute of Technology, Vietnam. He studies wireless network routing, security, and performance in edge computing, sensor networks, wireless mobile networks, and beyond 5G technologies. Assoc. Prof Dr. Trong-Minh Hoang is currently the head of the Telecommunication Network Department and a Senior EEE member.

Kumbesan SANDRASEGARAN (Senior Member, IEEE) received the Ph.D. degree in Electrical Engineering from McGill University, Canada, in 1994. He is working as an Associate Professor with the Chulalongkorn University, Thailand in 2024. His research interests include two main areas radio resource management in mobile networks, and engineering of remote monitoring systems for novel applications with industry through the use of embedded systems, sensors, and communications systems.